Research Article | Vol. 30, No. 14 / 4 Jul 2022 / Optics Express 25103
Optics EXPRESS

Dual electro-optic comb spectroscopy using a single pseudo-randomly driven modulator

VICENTE DURÁN,[1,*] CAMILO ESCOBAR-VERA,[2] MIGUEL SORIANO-AMAT,[2] HUGO F. MARTINS,[2,3] SONIA MARTIN-LOPEZ,[2] MIGUEL GONZALEZ-HERRAEZ,[2] AND MARÍA R. FERNÁNDEZ-RUIZ[2,3]

[1]*Institute of New Imaging Technologies, GROC-UJI, 12071 Castellón, Spain*
[2]*Universidad de Alcalá, Departamento de Electrónica, 28805 Alcalá de Henares, Spain*
[3]*Instituto de Óptica "Daza de Valdés" IO-CSIC, C/Serrano 121, 28006A Madrid, Spain*
[*]*vduran@uji.es*

Abstract: We present a dual-comb scheme based on a single intensity modulator driven by inexpensive board-level pseudo-random bit sequence generators. The result is a simplified architecture that exhibits a long mutual coherence time (up to 50 s) with no need of stabilization feedback loops or self-correction algorithms. Unlike approaches that employ ultrafast arbitrary waveform generators, our scheme makes it possible to produce long interferograms in the time domain, reducing the difference in the line spacing of the combs even below the hertz level. In order to check the system accuracy, we report two spectroscopic measurements with a frequency sampling of 140 MHz. All these results are analyzed and discussed to evaluate the potential of our scheme to implement a field-deployable dual-comb generator.

1. Introduction

Dual-comb spectroscopy (DCS) measures the spectral response of a sample by mapping an optical spectrum into the radio-frequency (RF) domain [1]. This frequency down-conversion is possible thanks to the interference of two optical frequency combs (OFCs) with different line spacing, in most cases only differing in a very small fraction. Even though DCS was devised using stabilized mode-locked OFCs, this technique has been progressively conducted with a variety of comb platforms [2–5]. Among them, OFCs that are generated by electro-optic (EO) modulation of a continuous-wave (cw) laser [6,7] turn into a very practical option when searching for a cost-effective and easily implementable DCS system. EO combs offer a wide range of comb line separations (covering several orders of magnitude, from megahertz to tens of gigahertz) and benefit from the high precision of the driving RF electronics. These features have led the EO approach to be adopted in applications other than spectroscopy, such as laser ranging and fiber sensing [8–10].

The possibility of generating a dual-comb spectrum by means of a single EO modulator has recently started to be explored [11,12]. The basic idea is to drive a Mach-Zehnder modulator (MZM) with a tailored multi-tone signal produced by an arbitrary waveform generator (AWG). The result is the creation, after a proper optical filtering, of a single-sided spectrum that is the sum of two combs with slightly different line spacing. The light emerging from this dual-comb generator is employed to interrogate a sample and then is directly photo-detected. The interference of the neighboring spectral lines that compose the optical spectrum produces a set of low-frequency beat notes, from which the sample amplitude response can be retrieved. Apart from its simplicity, such a "common-path" dual-comb approach provides a superior degree of mutual coherence when compared to a "two-arm" dual-comb interferometer, with no need of active stabilization mechanisms or correction algorithms. Indeed, long mutual coherence times (up to 50 s) have

#463604 https://doi.org/10.1364/OE.463604
Journal © 2022 Received 19 May 2022; accepted 31 May 2022; published 27 Jun 2022

Optics EXPRESS

been demonstrated when performing time-resolved DCS of a gas sample under a varying pressure [12].

The advantages and limitations of the above scheme are mainly linked to the AWG performance. On one hand, EO comb generation using an AWG makes it possible to arbitrarily tailor the shape of the output time-domain signals, avoiding the formation of high-peak-power pulses. This is beneficial for optimizing the signal-to-noise ratio (SNR) of the measured RF spectra. On the other hand, exploiting the bandwidths offered by high-speed MZMs (typically of a few tens of gigahertz) requires the AWG to have a sampling rate several times higher than the modulator bandwidth. For this reason, the systems so far reported involve ultrafast AWGs (with sampling rates of around 64×10^9 samples/s), often only available in advanced laboratories. Besides, the difference δf in the line spacing of the combs, which fixes the duration of a single interferogram (IGM), has a minimum value that is given by the ratio between the sampling rate and the AWG memory depth. Therefore, setting δf below 10 Hz implies very large memories, near or above 10^{10} samples. OFCs with so little difference in the line spacing are necessary in applications such as direct spectral dual-comb imaging [13–15], in which the data acquisition speed is eventually limited by the low number of frames per second of high resolution infrared cameras. This application may also benefit from the simplicity and robustness offered by a "common-path" DCS scheme. Additionally, ultradense combs with reduced line separations (~1 MHz or below), such as those used in sensing applications [16], require small values of δf to accommodate a large number of lines ($\sim 10^4$) inside the RF comb bandwidth.

In this paper, we propose a dual EO comb system that employs a single MZM driven by a combination of pseudo-random bit sequence (PRBS) signals obtained from inexpensive board-level generators. PRBS excitation to produce EO combs has already been applied to atomic and molecular spectroscopy, using, respectively, self-heterodyne detection [17] and the conventional two-arm dual-comb scheme [18]. In the latter case, the mutual coherence time can be increased above 1 s by offline data processing, with the aid of an IGM self-correction algorithm [19]. The one-arm system that we propose here not only simplifies the dual-comb architecture based on PRBS modulation but also provides a mutual coherence up to 50 s, similar to that previously demonstrated by a high-performance AWG [12]. In addition, the difference in the line spacing between the two generated OFCs can be easily reduced to very low values (even at the sub-hertz level). This configuration would require an extraordinarily large AWG memory depth, not widely available in the market. The performance of the implemented system is carefully analyzed and its capability to conduct spectroscopy is evaluated by means of two samples, namely, an athermal reference filter based on an etalon and a traceable hydrogen cyanide (HCN) gas cell. In the light of these results, the benefits and limitations of our approach are discussed, along with further developments.

2. Experimental results

2.1. Description of the setup

A basic sketch of our optical system is depicted in Fig. 1(a). As a light source, we employ a distributed feedback (DFB) semiconductor laser (SL) module (QDFBLD-1550-50, from QPhotonics), with a linewidth of ~5 MHz. It feeds a 20 GHz MZM (Optilab, IMC-1550-20-PM-HER), biased at its zero-transmission point [7]. This modulator is driven by the combined electrical signal provided by two similar PRBS evaluation boards, PRBS 1 and PRBS 2 (from Adsantec [20]) with a maximum bandwidth of 18 GHz. Both generators can produce, respectively, sequences of $2^7 - 1$ bits or $2^{15} - 1$ bits. For the spectroscopic measurements considered henceforth, we choose the first configuration. The clocking signals for the boards are obtained from synchronized frequency generators FG1 (Agilent, model N5183A) and FG2 (Hittite, model HMC-T2220), which create sinusoidal signals at f_{bit1} and f_{bit2}, respectively. The released bits streams are added in the electrical domain using a conventional RF power combiner and they are

Optics EXPRESS

boosted by a RF amplifier, RFA (ABP1800-03-3830, from Wenteq Microwave), before being sent to the MZM. The EO modulation of the laser light generates the optical spectrum shown in the inset of Fig. 1(a), formed by two interleaved OFCs with line separations f_s and $f_s + \delta f$. Each of these separations can be calculated as the corresponding bit frequency divided by the sequence length. Both OFCs share the central line (at the laser frequency f_0), so one side of the spectrum and the carrier must be removed by a band-pass filter (BPF), in order to guarantee a non-ambiguous frequency down-conversion. Ideally, only the spectral lines within the dashed line shown Fig. 1(a) should remain. However, due to the limited sharpness of the edges of a real BPF, a fraction of the usable spectrum is attenuated. The filtered OFC passes through a sample and is detected by a photodiode PD (New Focus, model 1811-FC). An RF low-pass filter (LPF) reduces the bandwidth of the detected signal, which is then digitized by an oscilloscope (Agilent, model DSO91304A). This digitizer and FG2 are both locked to the internal clock of FG1.

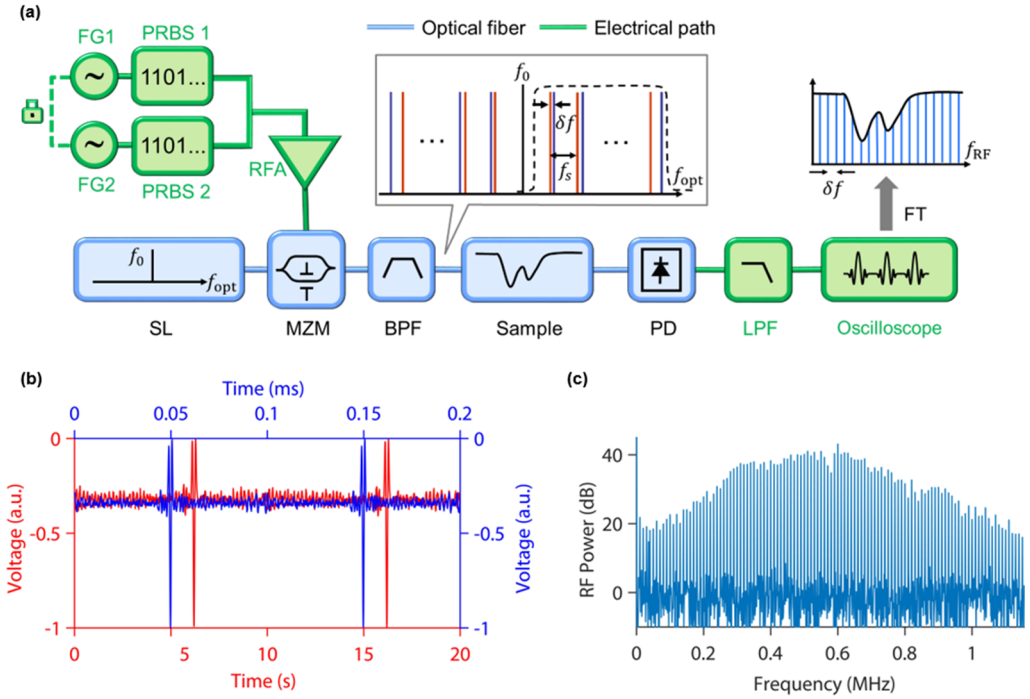

Fig. 1. (a) Sketch of the experimental setup for dual-comb spectroscopy using a single pseudo-randomly driven modulator. The central inset shows the optical spectrum created by the MZM (in this plot, f_{opt} denotes optical frequencies). After a proper filtering, the part of the spectrum outside the dashed line is ideally removed. By Fourier-transforming the time signal generated upon detection, we retrieve an RF comb with a line spacing δf (here, f_{RF} refers to RF frequencies) (b) Time-domain signals for δf = 10 kHz (blue curve composed of two 100-µs IGMs) and δf = 0.1 Hz (red curve composed of two 10-s IGMs). Both signals have been normalized and an arbitrary temporal shift has been introduced between them for the sake of comparison (c) RF comb spectrum of ten consecutive 100-µs IGMs, extending over a bandwidth of 1.14 MHz (114 lines separated by 10 kHz).

A Fourier transform (FT) analysis of the digitized signal leads to an RF comb with a line spacing δf [see the plot at the right side of Fig. 1(a)], so the compression factor is $f_s/\delta f$. To measure the sample spectral response, the recovered comb is normalized using an additional

Optics EXPRESS

spectrum obtained with no sample. This reference measurement is acquired by means of an auxiliary arm after the BPF [not shown in Fig. 1(a)], which ends in a second (twin) PD. In accordance with the theory of dual-comb interferometry, each IGM is, after a proper low-pass filtering, the cross-correlation between the comb signals [21]. Since the two employed PRBSs are similar, this cross-correlation results to be a periodic train of electrical pulses [22], with a repetition rate given by $1/\delta f_s$. The flexibility to vary the length of a single IGM by tuning the values of f_{bit1} and f_{bit2} can be observed in Fig. 1(b). The blue plot shows two consecutive IGMs, each one of a duration of 100 µs (δf = 10 kHz), while the red plot is a sequence of two 10-s IGMs (δf = 0.1 Hz). In both cases, the generated dual-comb spectrum is optically filtered by a tunable BPF (XTM-50, from Yenista). Since f_s = 140 MHz, the compression factor $f_s/\delta f$ goes from 1.4×10^4 to 1.4×10^9. In the case of using an AWG with a sampling rate of 64 GSa/s to drive the MZM, a difference in the line spacing of 0.1 Hz would require >500 GSa of memory depth [11], far beyond the typical values of commercially available devices. Figure 1(c) shows the RF comb spectrum obtained from a signal composed of 10 IGMs of 100 µs, covering a spectral window of 1.14 MHz, which corresponds to an optical bandwidth of around 16 GHz. By limiting this bandwidth to 10 GHz (72 lines), the power variation of the central part of the RF spectrum is reduced to less than 10 dB.

2.2. Signal-to-noise ratio analysis

To assess the degree of the mutual coherence of our system, we analyze the evolution of the spectral *SNR* as a function of the acquired signal length. As in [12], δf = 10 kHz and the oscilloscope has a sampling rate of 10 MSa/s and a memory of 500 MSa. Therefore, the duration of the longest signal that can be recorded is T = 50 s and contains $N = 5 \times 10^5$ IGMs. The frequencies that feed the PRBS generators are, respectively, f_{bit1} = 17.780 GHz and f_{bit2} = 17.78127 GHz, so f_s = 140 MHz. The *SNR* is calculated by dividing the amplitude of a RF line by the surrounding noise (that is, the noise in between lines) [18,21]. We extract series of consecutive elementary signals, which are aligned in time, averaged and Fourier-transformed. The *SNR* is then calculated by averaging over M = 114 lines (i.e., over 16 GHz of optical bandwidth). The result of this process can be observed in Fig. 2(a). The solid blue line is a nonlinear least squares fit of the experimental points assuming that the *SNR* scales as $\sqrt{N}$. The usual figure of merit for DCS, $FoM = SNR \times M \times T^{-1/2}$, achieves a value of 2×10^5 Hz$^{1/2}$, comparable to that previously reported when using two independent MZMs driven by PRBS generators [18]. The good agreement between the experimental points and the expected behavior in the *SNR* plot demonstrates that coherent averaging works well over the entire integration time. Eventually, it might fail due to the limited precision of the clock to which the signal generators are locked. To check it, we reduce δf to 1 kHz (f_{bit2} = 17.780127 GHz) and the sampling rate to 5 MHz to extend the integration time up to 100 s (exploiting again the maximum memory depth of our oscilloscope). The acquired signal is then formed by $N = 10^5$ IGMs of 1 ms. Figure 2(b) shows the evolution of the *SNR* in this second configuration. At 60 s, the experimental points start to clearly deviate from the expected tendency. By examining the acquired time signal, we observe that the sequence of IGMs shows a relative phase drift that degrades the coherent averaging [19,23]. Using a post-correction software based on the realignment and resampling of the IGMs, this effect can be corrected [see the red points in Fig. 2(b)]. In that case, our system can operate over a total integration time of 100 s, limited by the oscilloscope memory depth.

2.3. Spectroscopic measurements

As a first example of spectroscopic sample, we choose an athermal wavelength reference filter (from Primanex) based on an etalon that has a finesse $\mathcal{F}$ = 7 and a free spectral range FSR = 25 GHz. The optical filtering after the MZM is accomplished by means of a fiber Bragg grating (with a bandwidth of 0.11 nm) combined with the wavelength tuning mechanism of

Optics EXPRESS

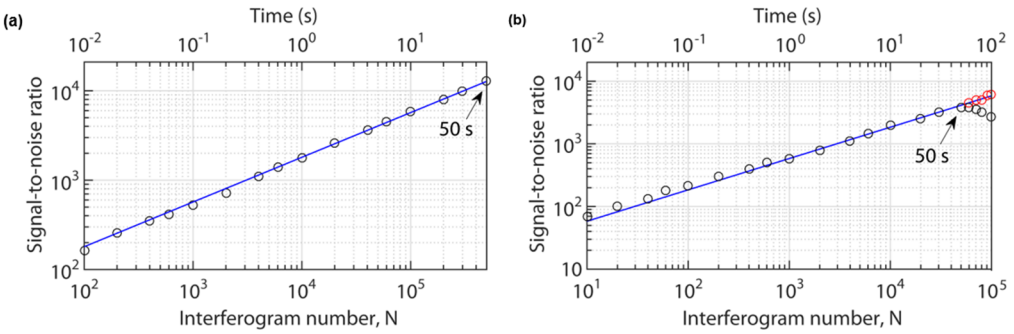

Fig. 2. Evolution of the spectral *SNR* as a function of total number of interferograms N or, alternatively, the integration time. The points are the measured *SNR* values and the solid line is a non-linear fit assuming that $SNR \propto \sqrt{N}$. (a) Results for $\delta f = 10$ kHz and an integration time of 50 s as in [12]. (b) Idem for $\delta f = 1$ kHz and an integration time of 100 s. The red points are corrected values obtained by post-processing software.

the DFB laser. The optical bandwidth in our reconstructions is chosen to be 10 GHz, which corresponds to the flattest part of our comb spectra. The difference in the line spacing of the combs is 1 kHz, the acquired signal is digitized at 20 MSa/s and its duration is 250 ms. The RF spectrum is normalized employing the reference measurement taken without the sample. Figure 3 shows the transmission curve as a function of the optical frequency detuning from the maximum of the resonance. The frequency axis is obtained by simply rescaling the corresponding RF values by a factor $f_s/\delta f$. The continuous line in Fig. 3 corresponds to the Airy distribution that better fits the experimental points [24]. This theoretical curve is obtained through a nonlinear least square fitting routine (based on the trust-region-reflective algorithm), assuming as initial values for $\mathcal{F}$ and FSR those given by the manufacturer. The corresponding residuals, shown in the plot below, have a root mean square (RMS) equal to 1%.

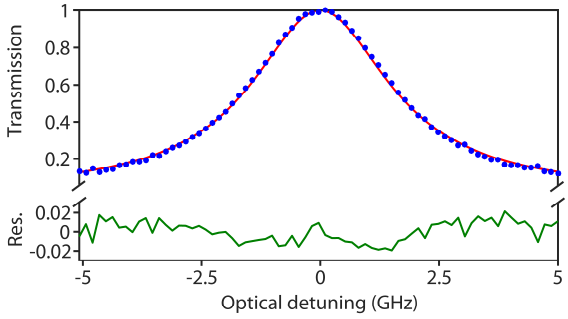

Fig. 3. Spectral response of an athermal filter based on an etalon obtained from a 250-ms signal. The experimental points (circle dots) are fitted by the theoretical curve for the transmission of a Fabry-Perot interferometer (red line). The corresponding residuals (Res.) are shown below.

As a second example of spectroscopic sample, we measure the transmission through a $H^{13}C^{14}N$ gas cell (from Wavelength References) with a pressure of 25 Torr and a length of 5.5 cm. The

Optics EXPRESS

BPF is the tunable bandpass filter (XTM-50), configured to enable the measurement of the ro-vibrational transition P10 in the vicinity of 1549.73 nm. Figure 4(a) shows the absorption line over 10 GHz of optical bandwidth. This result is obtained from a 1-s trace composed of 10^3 IGMs (δf = 1 kHz), digitized with a sampling rate of 20 MSa/s. As before, the curve is obtained through a normalization process using the reference measurement (without cell). The continuous line in Fig. 4 is the Voigt profile that fits the recovered values. The residuals between the theoretical and experimental points do not exhibit any systematic deviation and have an RMS of 0.26%. The minimum transmission is 0.17 lower than that of the points separated by 5 GHz from the center of the line. This result is consistent with the data provided by NIST for the HCN [25].

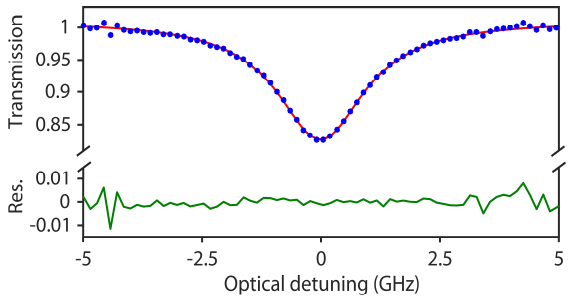

Fig. 4. Measurement of the HCN line P10 over 10 GHz of optical bandwidth with a point spacing of 140 MHz. This reconstruction is obtained from a 1-s signal when the difference in the line spacing of the combs is δf = 1 kHz. The experimental points are fitted by a Voigt profile (red line) and the corresponding residuals (Res.) are shown below.

3. Discussion and conclusion

In conclusion, we have presented a common-path dual-comb approach based on pseudo-random modulation that employs a single MZM. The driving RF signal is generated from a couple of inexpensive PRBS evaluation boards. The result is a scheme that provides a high mutual coherence at a time scale close to one minute. This value is similar to that previously reported using much more expensive RF equipment [12] and it is remarkably better than the mutual coherence of a free-running EO-DCS system with two comb generators fed by a single laser. Since the "common-path" approach does not require an exceptionally high coherence light source, a seed laser with a modest linewidth (here, ~ 5 MHz) can be employed. These advantages are at the cost of some limitations when compared to an approach based on an ultrafast AWG. Our system does not enable a control of the spectral phase of the combs to optimize the *SNR*, although the use of binary sequences within one period helps limit the peak-to-average power ratio [11,12]. On the other hand, given an optical bandwidth, the comb line spacing depends on the number of bits within one PRBS. For our generators, that number is limited to only a couple of values, which restricts the flexibility in choosing the number of lines M. However, our setup allows us to largely control and expand the length of a single interferogram ($1/\delta f$) by just reconfiguring one of the PRBS generators. As in other dual-comb schemes, the maximum attainable δf is given by $f_s/(2M)$, where M can be calculated as the optical bandwidth BW_{opt} of the combs divided by f_s [26]. When using a pseudo-random modulation, f_s is given by the bit frequency f_{bit} (which can be set to match the maximum bandwidth of the PRBS generators) divided by the number of bits, $f_s = f_{bit}/(2^n - 1)$. For our setup, $f_{bit} \cong 18$ GHz, $n = 7$ and $BW_{opt} = 16$ GHz,

Optics EXPRESS

so $\delta f_{max} \cong$ 600 kHz. The minimum value of δf, on its turn, is only restricted by the mutual coherence of the combs. Concretely, a difference in the line spacing as low as 0.1 Hz has been demonstrated here, far below the minimum values previously reported by a dual-comb system based on a single MZM (200 Hz in [11] and 32 Hz in [12]). As explained, this distinctive feature can be especially beneficial for applications such as direct dual-comb imaging, since this technique relies on pixelated sensors with typical refresh rates of tens or hundreds of frames per second (see, for instance, [13]). Also, in the case of configuring our system to produce an ultradense comb composed of $\sim 3 \times 10^4$ lines separated by around 550 kHz (by using sequences of $2^{15} - 1$ bits), accommodating all the lines within 275 kHz would require $\lesssim$ 10 Hz. In terms of spectroscopic performance, the *FoM* of our system is comparable to that previously reported with two independent MZMs driven by pseudo-random modulation, but the mutual coherence in our case is much longer when using raw data [18]. Other easily implementable dual-comb schemes based on electro-optic or acousto-optic modulators have similar *FoM* (for $f_s \sim$ 100 MHz) but with worse mutual coherence (commonly constrained to a time scale <1 s) if no stabilization loops are added to the system [3,27].

In addition to the above benefits, there is still room for further developments. In our experiments, the implemented setup includes a high-performance oscilloscope, but the efficient down-conversion provided by the generated combs permits the use of a low-bandwidth digitizer (~10 MSa/s). On the other hand, the benchtop RF signal generators that produce the bit frequencies could be easily replaced by low-cost and low-noise frequency synthesizers at a reduced cost. In terms of bandwidth, commercially available PRBS evaluation boards offer frequency ranges of 30-40 GHz (2× the bandwidth demonstrated here) and the number of bits (an consequently, the number of comb lines) can be chosen between 2^7 and 2^{15} [20]. By employing dedicated filters to take advantage of both sides of the generated spectrum (one for probing a sample and the other for the reference measurement), the optical bandwidth might be extended to at least 2×30 GHz. This would increase by 5/3 the widest dual-comb spectrum previously reported with such a filtering configuration [12]. In addition, by selecting generators with a proper number of bits, the line spacing of the combs could be adapted to the targeted application (from ~ 100 MHz to the sub-MHz level). For all this, the presented approach offers a simple solution for the implementation of a robust, inexpensive and versatile dual-comb instrument, with the potential of being exploited outside the laboratory environment in spectral imaging of molecular resonances and sensing applications.

Funding. Comunidad de Madrid and FEDER program (P2018/NMT-4326); Generalitat Valenciana (PROMETEO/2020/029); Universitat Jaume I (UJI-B2019–45); Ministerio de Ciencia e Innovación (MCIN/AEI/10.13039/501100011033, RTI2018–097957-B-C31, RTI2018–097957-B-C32, RTI2018–097957-B-C33); European Union Next Generation EU/PRTR program (PSI ref. PLEC2021-007875).

Acknowledgments. V.D., M.S.A., and M.R.F.R. acknowledge financial support from the Spanish MICINN under contract no. RYC-2017–23668, PRE-2019–087444, and IJC2018–035684-I, respectively. Also, this work has been partially funded by the Spanish Ministry of Science and Innovation MCIN/AEI/10.13039/501100011033 and by the European Union Next Generation EU/PRTR program, under project PSI ref. PLEC2021-007875.

Disclosures. The authors declare no conflicts of interest.

Data Availability. The data underlying the results presented in this paper are not publicly available at this time but may be obtained from the authors upon reasonable request.

References

1. I. Coddington, W. C. Swann, and N. R. Newbury, "Coherent multiheterodyne spectroscopy using stabilized optical frequency combs," *Phys. Rev. Lett.* **100**(1), 013902 (2008).
2. D. A. Long, A. J. Fleisher, K. O. Douglass, S. E. Maxwell, K. Bielska, J. T. Hodges, and D. F. Plusquellic, "Multiheterodyne spectroscopy with optical frequency combs generated from a continuous-wave laser," *Opt. Lett.* **39**(9), 2688–2690 (2014).
3. V. Durán, L. Djevarhidjian, and H. G. de Chatellus, "Bidirectional frequency-shifting loop for dual-comb spectroscopy," *Opt. Lett.* **44**(15), 3789–3792 (2019).

Optics EXPRESS

4. M.-G. Suh, Q.-F. Yang, K. Y. Yang, X. Yi, and K. J. Vahala, "Microresonator soliton dual-comb spectroscopy," Science **354**(6312), 600–603 (2016).
5. C. Quevedo-Galán, V. Durán, A. Rosado, A. Pérez-Serrano, J. M. G. Tijero, and I. Esquivias, "Gain-switched semiconductor lasers with pulsed excitation and optical injection for dual-comb spectroscopy," Opt. Express **28**(22), 33307–33317 (2020).
6. V. Torres-Company and A. M. Weiner, "Optical frequency comb technology for ultra-broadband radio-frequency photonics," Laser Photon. Rev. **8**(3), 368–393 (2014).
7. A. Parriaux, K. Hammani, and G. Millot, "Electro-optic frequency combs," Adv. Opt. Photonics **12**(1), 223–287 (2020).
8. H. Wu, T. Zhao, Z. Wang, K. Zhang, B. Xue, and J. Li, "Long distance measurement up to 1.2 km by electro-optic dual-comb interferometry," *Appl. Phys. Lett.* **111**(25), 251901 (2017).
9. E. L. Teleanu, V. Durán, and V. Torres-Company, "Electro-optic dual-comb interferometer for high-speed vibrometry," Opt. Express **25**(14), 16427–16436 (2017).
10. M. Soriano-Amat, H. F. Martins, V. Durán, L. Costa, S. Martin-Lopez, M. Gonzalez-Herraez, and M. R. Fernández-Ruiz, "Time-expanded phase-sensitive optical time-domain reflectometry," Light Sci. Appl. **10**(1), 51 (2021).
11. M. Soriano-Amat, M. A. Soto, V. Durán, H. F. Martins, S. Martin-Lopez, M. Gonzalez-Herraez, and M. R. Fernández-Ruiz, "Common-Path Dual-Comb Spectroscopy Using a Single Electro-Optic Modulator," J. Light. Technol. **38**(18), 5107–5115 (2020).
12. J. H. Huh, Z. Chen, E. Vicentini, T. W. Hänsch, and N. Picqué, "Time-resolved dual-comb spectroscopy with a single electro-optic modulator," *Opt. Lett.* **46**(16), 3957–3960 (2021).
13. P. Martín-Mateos, F. U. Khan, and O. E. Bonilla-Manrique, "Direct hyperspectral dual-comb imaging," Optica **7**(3), 199 (2020).
14. T. Voumard, T. Wildi, V. Brasch, R. G. Álvarez, G. V. Ogando, and T. Herr, "AI-enabled real-time dual-comb molecular fingerprint imaging," *Opt. Lett.* **45**(24), 6583–6586 (2020).
15. F. Ullah Khan, G. Guarnizo, and P. Martín-Mateos, "Direct hyperspectral dual-comb gas imaging in the mid-infrared," *Opt. Lett.* **45**(19), 5335–5338 (2020).
16. Y. Bao, X. Yi, Z. Li, Q. Chen, J. Li, X. Fan, and X. Zhang, "A digitally generated ultrafine optical frequency comb for spectral measurements with 0.01-pm resolution and 0.7-μs response time," Light Sci. Appl. **4**(6), e300 (2015).
17. N. B. Hébert, V. Michaud-Belleau, J. D. Anstie, J. D. Deschênes, A. N. Luiten, and J. Genest, "Self-heterodyne interference spectroscopy using a comb generated by pseudo-random modulation," Opt. Express **23**(21), 27806–27818 (2015).
18. K. Fdil, V. Michaud-Belleau, N. B. Hébert, P. Guay, A. J. Fleisher, J. D. Deschênes, and J. Genest, "Dual electro-optic frequency comb spectroscopy using pseudo-random modulation," *Opt. Lett.* **44**(17), 4415–4418 (2019).
19. N. B. Hébert, V. Michaud-belleau, J. Deschênes, and J. Genest, "Self-Correction Limits in Dual-Comb Interferometry," *IEEE J. Quantum Electron.* **55**(4), 1–11 (2019).
20. "Adsantec, Advanced Science and Novel Technology Co., Inc." [Online]. Available: https://www.adsantec.com/categories/board-level-products/.
21. N. R. Newbury, I. Coddington, and W. Swann, "Sensitivity of coherent dual-comb spectroscopy," Opt. Express **18**(8), 7929–7945 (2010).
22. K. Fdil, V. Michaud-Belleau, N. B. Hébert, and J. Genest, "Dual electro-optic comb spectroscopy using quadrature demodulation," in *Optical Sensors and Sensing Congress*, OSA Technical Digest, 2020, p. EM2C.4.
23. P. Guay, J. Genest, and A. J. Fleisher, "Precision spectroscopy of $H^{13}CN$ using a free-running, all-fiber dual electro-optic frequency comb system," *Opt. Lett.* **43**(6), 1407–1410 (2018).
24. B. E. A. Saleh and M. C. Teich, *Fundamental of Photonics*, 3rd ed. John Wiley & Sons, 2019.
25. "NIST, SRM 2519a." [Online]. Available: https://www-s.nist.gov/srmors/view_detail.cfm?srm=2519A.
26. I. Coddington, N. Newbury, and W. Swann, "Dual-comb spectroscopy," Optica **3**(4), 414–426 (2016).
27. A. J. Fleisher, D. A. Long, Z. D. Reed, J. T. Hodges, and F. Plusquellic, "Coherent cavity-enhanced dual-comb spectroscopy," Opt. Express **24**(10), 10424–10434 (2016).